



HAL
open science

Assessment of the triangle method (T-VI) for detection of water leaks from airplane and UAV

Jean-Claude Krapez, Javier Sanchis Muñoz, Christian Chatelard, Christophe Mazel, Vincent Olichon, Juan Barba Polo, Yves-Michel Frédéric, Eric Coiro, Duarte Carreira, Alexandra Carvalho

► **To cite this version:**

Jean-Claude Krapez, Javier Sanchis Muñoz, Christian Chatelard, Christophe Mazel, Vincent Olichon, et al.. Assessment of the triangle method (T-VI) for detection of water leaks from airplane and UAV. IGARSS 2020 IEEE International Geoscience and Remote Sensing Symposium, Sep 2020, Virtuel, United States. hal-03071642

HAL Id: hal-03071642

<https://hal.science/hal-03071642v1>

Submitted on 16 Dec 2020

HAL is a multi-disciplinary open access archive for the deposit and dissemination of scientific research documents, whether they are published or not. The documents may come from teaching and research institutions in France or abroad, or from public or private research centers.

L'archive ouverte pluridisciplinaire **HAL**, est destinée au dépôt et à la diffusion de documents scientifiques de niveau recherche, publiés ou non, émanant des établissements d'enseignement et de recherche français ou étrangers, des laboratoires publics ou privés.

ASSESSMENT OF THE TRIANGLE METHOD (T-VI) FOR DETECTION OF WATER LEAKS FROM AIRPLANE AND UAV

*J.-C. Krapez¹, J. Sanchis Muñoz², C. Chatelard¹, C. Mazel³, V. Olichon³, J. Barba Polo²,
Y.-M. Frédéric¹, E. Coiro¹, D. Carreira⁴, A. Carvalho⁴*

¹ ONERA The French Aerospace Lab, 13300 Salon de Provence, France

² Galileo Geosystems, Manises 46940, Valencia, Spain

³ Air Marine, 33850 Leognan, France

⁴ EDIA, 7800 Beja, Portugal

Corresponding author: krapez@onera.fr

ABSTRACT

Water leak detection in water transportation mains outside urban areas by airborne remote sensing has been assessed with a series of measurement campaigns in 2017 and 2018 over SCP (Société du Canal de Provence – France) network. The most appropriate equipment for revealing high moisture areas and artificial leaks coming from the image database (VNIR, TIR spectral range) allowed us to validate the choice of the onboard instrumentation for both types of platforms (manned & unmanned) associated with the multispectral approach (Triangle method). This work aims to validate further the water leak detection technique developed in the WADI project. This was performed in the framework of a new airborne campaign in May and September 2019 over EDIA (Empresa de Desenvolvimento e Infra-estruturas do Alqueva – Portugal) network with a plane and an UAV in operational environment.

1. INTRODUCTION

Water has become increasingly scarce and less predictable. For this reason, water loss in the transmission networks represents a waste of limited natural resources and is then a perennial problem which challenges the efficiency of water transmission systems.

Currently, active leakages in water distribution networks are detected and located by ground sensing and monitoring techniques based on the measurement of pressure differences, acoustic sounding and ground penetrating radar. These ground methods become difficult or inadequate for water transmission mains, especially out of urban areas, and for open canals. New efficient and cost-effective pipeline surveillance methods are thus required.

Depending on the severity of the pipe damage, the excess of water supplied by the leak can reach the ground surface by diffusion and capillarity. On the other side the water supplied by the leak will benefit to the vegetation that

is already present or induce the growth of opportunistic plants. All this contributes to modify the optical properties of the surface, namely the reflectance (a visible effect associated to soil moisture increase is surface darkening) as well as the thermal properties of the upper soil layer. On the other side, an increase of soil moisture induces changes in thermal emission related to changes in both infrared emissivity and temperature. Temperature variations can be due to increased evaporation and transpiration (latent heat losses between soil/vegetation and atmosphere) and/or increased thermal inertia of the soil but also of the different elements of the watered vegetation (leaves, branches). As a matter of fact, all these effects contribute to reduce the day-night amplitude of the temperature variations. Wet areas should show a lower temperature as compared to drier areas during sunny day hours, whereas the opposite is expected after the sunset and before the dawn [1].

Excess of water in the soil as induced by a leak, because of its consequences on the optical properties (visible and near infrared reflectance) as well on the thermal radiation of both soil and vegetation surfaces should be detectable by the use of airborne optical remote sensing in optical bands and thermal bands.

Thermal infrared (TIR) sensors are used on this basis to assess the soil moisture or the evaporation rate over vegetation canopy areas [2-9]. However, the detection accuracy of the TIR [2, 3, 7] is low leading to false positives and misinterpretations caused by diverse scenarios like dense vegetation or shadows. To overcome this limitation, TIR was combined with visible and NIR data from multispectral or hyperspectral cameras [4, 6, 8, 9]. A combined use of TIR and VIS-NIR data like in the Triangle Method can be used in water leak detection over water transmission pipes and canals to gain accuracy. This method consists in combining the apparent temperature and a vegetation index like NDVI to perform a temperature-VI scatterplot for all the pixels over an area with a wide diversity in terms of cover fraction and water content. The

name is related to the (roughly) triangle shape of the obtained scatterplot [10-17]. Actually, the vertex of the triangle is often truncated, giving a trapezoidal shape. The scatterplot yields to the calculation of a water index for each point or pixel by making a quotient between its relative position with respect to the dry edge and the wet edge of the triangle/trapezoid [10-17].

An airborne remote sensing campaign was conducted during February, April and July 2017, south of France, over several areas of SCP water network infrastructure, to evaluate the applicability of the temperature/Vegetation Index space (i.e. the triangle/trapezoid method) in a water leak detection method based on airborne data. The campaigns were performed with ONERA's aerial platform BUSARD. It was instrumented with two hyperspectral cameras in the VNIR and SWIR spectrum (Hypex) and a microbolometer infrared camera (FLIR A325 or FLIR A655sc 7.5-12 μ m). The best results were obtained by applying the triangle method while combining a thermal infrared image and a vegetation index image built from two images in the visible and NIR range [18]. Upon selecting the most appropriate wavelengths, two platforms (manned airplane and UAV) have been equipped with corresponding instruments which constitutes the WADI technique [19]. The method was then validated at different scales by operating simultaneously the manned aircraft platform and the UAV in October 2018 over an area with artificial leaks [20].

The aim of this work is to validate further the WADI technique with data acquired in May and September 2019 over real and artificial leaks of the water transportation network of EDIA in Portugal.

2. MATERIALS AND METHODS

The aircraft (MAV) was a Tecnam P2006T operated by Air Marine and instrumented with a Spectrocam VNIR multispectral camera (with filters at 660 nm and at 832.5 nm), a Noxant thermal infrared (TIR) cooled camera (7.7 – 9.3 μ m) and a custom made acquisition software. The flights with the manned platform were performed at an altitude of 800 m which led to a spatial resolution of 0.30 m for the VNIR camera and 0.48 m for the TIR camera.

The UAV was a custom designed multicopter operated by Galileo Geosystems and instrumented with a Micasense RedEdge 3 VNIR multispectral camera (with five bands: 475, 560, 668, 717 and 840 nm) and a microbolometer uncooled FLIR Vue Pro R TIR camera (7.5 – 13.5 μ m). The flights with the unmanned platform were performed at an altitude of 50 m which led to a spatial resolution of 3.4 cm for the Micasense camera and 6.5 cm for the FLIR camera. Soil moisture ground measurements have been carried out during the flights in the 5 cm upper layer with a portable FDR probe over the area of interest to assess the results.

In the present work three bands have been used in both cases, manned aircraft and UAV: 660 nm (red), 832,5 nm

(NIR) and TIR for manned aircraft and 668 nm (red), 840 nm (NIR) and TIR for UAV. The multispectral aircraft data are uncalibrated raw data. On the other hand, a radiometric calibration based on a Spectralon target has been applied as part of the radiometric calibration carried out by Pix4D in the case of the red and NIR bands of the UAV acquired data. Besides, although the aircraft and the UAV TIR cameras have been both radiometrically calibrated, the emissivity parameter has been set to 1 and no correction has been applied to the raw data to extract the true temperature from the brightness temperature. As a matter of fact, the work in [18] has shown negligible differences in the resulting wetness index whether using calibrated or uncalibrated remote sensing data.

The rest of the data processing pipeline is similar in both cases. The images have been pre-processed with the Pix4D photogrammetric software to obtain spectral orthomosaics. Then, the spectral mosaics have been normalized while excluding possible outliers. The co-registration of the spectral orthomosaics has been done with Gefolki software developed by ONERA [21] and Pix4D (only the UAV multispectral data). The co-registration has been done taking as master the TIR image as the lowest resolution image in both cases; for this purpose a resampling of the VNIR with a bi-cubic spline interpolation algorithm was performed.

The empirical Triangle/Trapezoid method according to [10] can be implemented by using either NDVI or OSAVI for the vegetation index (VI). OSAVI is likely to show better immunity to variations in bare soil reflectance thus being better correlated with the cover fraction [22]. The water index (WI) is obtained by first reporting each pixel of the scene in the temperature – VI space. The resulting T-VI scatterplot shows a triangle/trapezoid shape. The WI of a pixel is calculated according the next expression:

$$WI = \frac{T_{dry} - T_{TIR}}{T_{dry} - T_{wet}} \quad (1)$$

where T_{TIR} is the temperature of the pixel, whereas T_{wet} and T_{dry} are the lowest and highest temperatures observed at the same VI as the considered pixel. The lowest one, T_{wet} , belongs to the so-called “cold” edge (or “wet” edge”) of the triangle/trapezoid distribution, whereas the highest one, T_{dry} , belongs to the “warm” edge (or “dry” edge). In the classical Triangle method these edges are chosen to be straight lines. They can be set automatically or manually, although the best results have been obtained by setting the edges manually. A software called WadiLeaks has been developed by Galileo Geosystems to carry out all the processing steps in a unique graphical user interface.

3. RESULTS

The area of study in the present work is within EDIA's network. The block 2 of Monte Novo site located in Sao Manços (Evora, Portugal) has been selected for a high

percentage of metallic pipes and a high probability of leaks to occur. An airborne campaign was performed in May 2019 and, in addition to artificial leaks, a real water leak was revealed after analyzing the aircraft images: a slight contrast could indeed be observed in the WI images from the manned platform. Local ground leak detection with acoustic sensors implemented by EDIA in June, confirmed a high probability of leakage on the H5 pipe near the suspected area.

A flight on this area was planned and performed in September 2019 with both the MAV & UAV platforms. A ground truth measurement, carried out simultaneously, has shown that the mean moisture level was about 13% along the leak area while reaching locally 23%, whereas it was only about 7% a few meters aside. Sparse green vegetation (short grass) could be seen along the leak area, as opposed to dry vegetation away from it.

The OSAVI images obtained from the VIS and NIR images acquired onboard the airplane and the UAV are reported in Fig. 1. Notice that the flight line of the airplane was much larger than the image represented in Fig. 1-left. The latter has itself a much larger extent than the area covered by the UAV (Fig. 1-right, whose size is reported by a black rectangle in the left image). In return, the spatial resolution obtained by the UAV sensors is from 7 to 9 times better.

The Temperature-VI scatterplots obtained with the two sets of sensors are reported in Fig. 2. The observed differences have different origins. First, since the airplane explored a wider region, the corresponding scatterplot is expected to cover a wider range of values for both (absolute) OSAVI and (absolute) temperature. On the other side, due to the lack of calibration of the VNIR bands from the manned aircraft, and due to separate normalization of OSAVI and temperature from both sets of instruments, a direct comparison is not possible, although this does not affect the leaks' detection methodology.

For each scatterplot, the wet edge (low temperature border) and the dry edge (high temperature border) have been set manually, by excluding only a small number of pixels (outliers). The pixels that are excluded at bottom right of the scatterplot from the manned aircraft data correspond to roads and paths.

In the end, the inferred water index (WI) maps are reported in Fig. 3. The color scale is such that high moisture areas are in dark blue whereas low moisture areas are in light blue or even in white.

The WI contrast revealing the leak as observed by the manned platform in May 2019 appeared in Sept 2019 as well, on both WI images, from manned platform and from UAV although with different amplitudes. Although rather small, the contrast related to the leak is quite satisfactory thanks to the fact that the weather was warm and dry (end of summer) and to the fact that vegetation was absent or very small (the harvest was made in June).

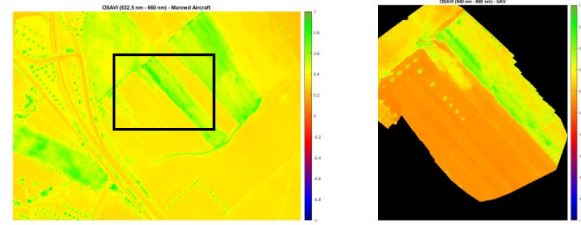


Fig. 1. OSAVI vegetation index map obtained with the manned aircraft (left) and with the UAV (right). The area covered by the UAV in the right image corresponds approximately to the black rectangle in the left image. The OSAVI scales are different.

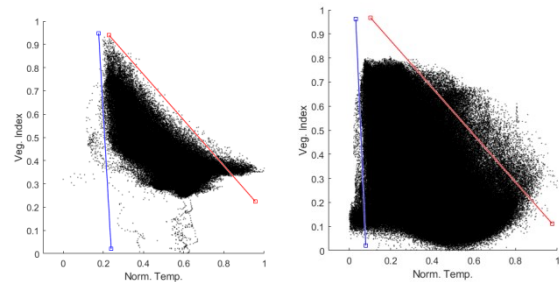


Fig. 2. 2D scatterplots of the Vegetation Index (OSAVI) vs. the normalized brightness temperature as obtained from the manned aircraft (left) and from the UAV (right). The wet edge is in blue and the dry edge is in red.

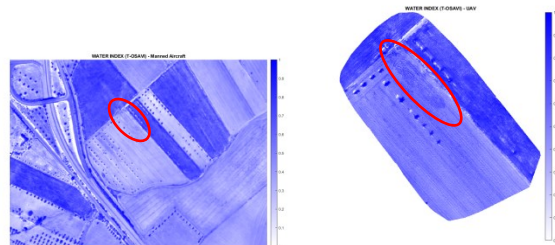


Fig. 3. Water index (WI) from the manned aircraft (left) and from the UAV (right). The real leakage area is highlighted with a red ellipse.

These are conditions that increase the probability of detection of water leaks against other sources of reflectance or temperature variations (as for example high vegetation, shadows, recent precipitation, humid air ...).

A multitemporal analysis has been performed with the UAV. In Fig. 4 to 6 are reported the images of OSAVI, brightness temperature and water index (WI) recorded at 16h, at 18h, and just after sunset at 20h. The vegetation index is expected to be constant, yet, due to low signals after sunset, a bias (global decrease) is observed (Figs 4, 5, 6 at left). On the other side, the temperature (negative) contrast over the leak area progressively decreases with time (Figs 4, 5, 6 in the middle). At sunset, it has nearly disappeared. This makes that the water index (positive) contrast disappears as well (Figs 4, 5, 6 at right). Due to competing influences between VI and temperature variations, it seems that the WI contrast is not monotonically decreasing but shows a maximum at 18h. However, at this late time, one faces adverse effects like tree shadows (see Fig. 5). Moreover, this finding cannot be generalized at present stage since the

considered area was too small for building a well populated scatterplot as required in the Triangle method. More work is needed to evaluate precisely at which time a leak signature is revealed at best.

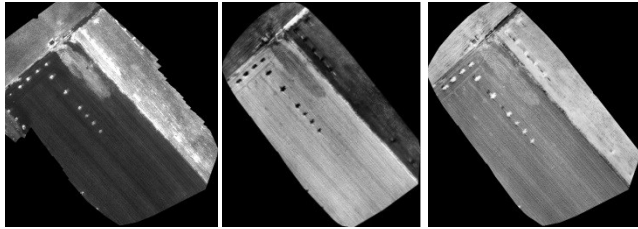


Fig. 4. Results obtained with UAV at 16h. OSAVI (left) Temperature (middle), inferred Water index (right).

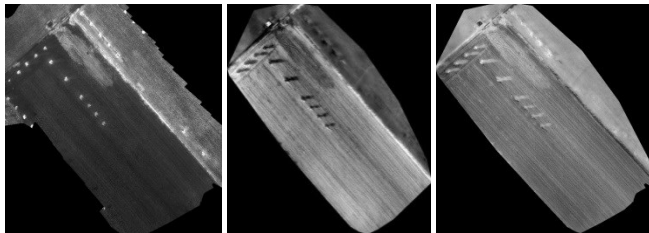


Fig. 5. same at 18h.

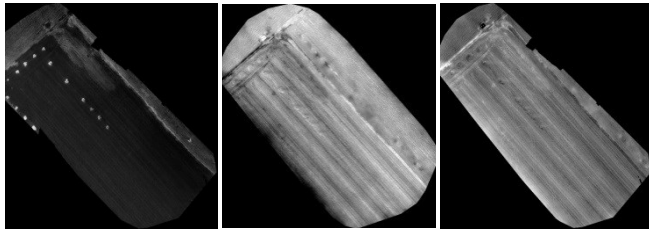


Fig. 6. same at 20h.

4 CONCLUSION

An airplane and UAV remote sensing campaign was performed in May and September 2019 over EDIA water transportation means for validating in operational conditions the WADI system aimed to detecting water leaks. In the Monte-Novo site, both artificial and natural leaks were present. The multispectral “triangle” method has been applied with both systems to reach complementary performances regarding field scale and resolution. A preliminary multitemporal analysis showed that there was a way to optimize the leak signature by playing on the time of flight with respect to sun radiance history.

After the irrigation period, the pipe H5 will be checked for repair by the Portuguese water company EDIA.

ACKNOWLEDGEMENT

This work has been supported by the EU-funded H2020 project WADI - Water-tightness Airborne Detection Implementation (www.waditech.eu) under grant agreement No 689239.

REFERENCES

- [1] V. I. Myer, Crops and soils. In *Manual of Remote Sensing*, American Society of Photogrammetry, Falls Church, Virginia, (1975) 1715-1813.
- [2] M.D. Nellis, Application of thermal infrared imagery to canal leakage detection, *Remote Sens. Environ.*, 12 (1982) 229-234.
- [3] J.P. Tracey, P.A. Walton, Hydrologic investigations in canal and aqueduct systems using airborne thermal infrared line scanning, *In Geoscience and Remote Sensing Symposium, IGARSS'89 12th Canadian Symposium on Remote Sensing*, vol. 5, IEEE (1989) 2815-2819.
- [4] J.M. Pickerill, T.J. Malthus, Leak detection from rural aqueducts using airborne remote sensing, *Int. J. of Remote Sens.* 19 (1998) 2427-2433.
- [5] I.J. McGowen, S.L. Duff, I. Smith, Identifying channel seepage using pre-dawn thermal imagery, *In Geoscience and Remote Sensing Symposium, IGARSS'01*, 4, IEEE (2001) 1631-1633.
- [6] Y. Huang, G. Fipps, S.J. Maas, R.S. Fletcher, Airborne remote sensing for detection of irrigation canal leakage, *Irrig. Drain.*, 59 (2009) 524-534.
- [7] S.J. Thomson, C. Ouellet-Plamondon, S.L. DeFauw, Y. Huang, D.K. Fisher, P.J. English, Potential and challenges in use of thermal imaging for humid region irrigation system management, *J. Agric. Sci.* 4, (2012) 103.
- [8] M. Arshad, R. Gomez, A. Falconer, W. Roper, M. Summers, A remote sensing technique detecting and identifying water activity sites along irrigation canals, *Am. J. Envir. Eng. & Sci.* 1 (2014) 19-35.
- [9] S.L. Cundill, M. Meijde, R.G.K. Hack, Investigation of remote sensing for potential use of dike inspection, *IEEE J. Sel. Top. Appl. Earth Obs. Rem. Sens.*, 7 (2014) 733-746.
- [10] I. Sandholt, K. Rasmussen, J. Andersen, A simple interpretation of the surface temperature-vegetation index space for assessment of surface moisture status, *Remote Sens. Environ.* 79 (2002) 213-224.
- [11] T.N. Carlson, An overview of the “triangle method” for estimating surface evapotranspiration and soil moisture from satellite imagery, *Sensors*, 7 (2007) 1612-1629.
- [12] G. P. Petropoulos, G. Ireland, B. Barrett, Surface soil moisture retrievals from remote sensing: Current status, products & future trends. *Physics and Chemistry of the Earth, Parts A/B/C*, 83, (2015) 36-56.
- [13] J.-C. Krapez, A. Olioso, B. Coudert, Comparison of three methods based on the temperature-NDVI diagram for soil moisture characterization, *Proc. of SPIE* 7472, 74720 (2009) 1-12.
- [14] J.-C. Krapez, A. Olioso, A combination of temperature, vegetation indexes and albedo, as obtained by airborne hyperspectral remote sensing, for the evaluation of soil moisture, *J. Quant. Infr. Thermogr.*, 8 (2011) 187-200.
- [15] J.-C. Krapez, C. Chatelard, J.-F. Nouvel, P. Déliot, Combined airborne thermography and visible-to-near infrared reflectance measurement for soil moisture mapping, *QIRT 2012 Conference*, 11-14 June 2012, University of Naples Federico II, Naples, Italy.
- [16] A. Maltese, C. Cammalleri, F. Capodici, G. Ciraolo, G. L. Loggia, Surface soil humidity retrieval using remote sensing techniques: a triangle method validation, *Proc. of SPIE* 7824, 782425, (2010) 1-8.
- [17] A. Maltese, F. Capodici, G. Ciraolo, G. L. Loggia, Soil water content assessment: Critical issues concerning the operational application of the triangle method, *Sensors*, 15 (2015) 6699-6718.
- [18] C. Chatelard, J.-C. Krapez, P. Barillot, P. Déliot, Y.-M. Frédéric, J. Pierro, J.-F. Nouvel, F. Hélias, Y. Louvet, I. Legoff, G. Serra, “Multispectral approach assessment for detection of losses in water transmission systems by airborne remote sensing”, *HIC 2018*, 13th Int Conf. Hydrodynam., Palermo (It).
- [19] European Commission. WADITECH, Innovative Airborne Water Leak Detection Surveillance Service, <http://www.waditech.eu>
- [20] C. Chatelard, J. Sanchis Muñoz, J.-C. Krapez, C. Mazel, V. Olichon, J. Barba Polo, Y.-M. Frédéric, F. Hélias, P. Barillot, I. Legoff, G. Serra, “Multispectral approach validation for leak detection in water transmission systems by airborne remote sensing”, *IGARSS2019*, Yokohama (Jap).
- [21] G. Brigot, E. Colin-Koeniguer, A. Plyer, F. Janez, Adaptation and evaluation of an optical flow method applied to coregistration of forest remote sensing images, *IEEE J. Sel. Topics Appl. Earth Obs. Rem. Sensing*, 9 (2016) 2923-2939.
- [22] G. Rondeaux, M. Steven, F. Baret, Optimization of soil adjusted vegetation indices, *Remote Sens. Environ.*, 55 (1996) 95-107.